Buckling load optimization of beam reinforced by nanoparticles

Mohsen Motezaker[1*] and Arameh Eyvazian[2]

[1]*School of Railway Engineering, Iran University of Science and Technology, Tehran, Iran*
[2]*Mechanical and Industrial Engineering Department, College of Engineering, Qatar University, P.O. Box 2713, Doha, Qatar*

Abstract.   This paper deals with the buckling and optimization of a nanocomposite beam. The agglomeration of nanoparticles was assumed by Mori-Tanaka model. The harmony search optimization algorithm is adaptively improved using two adjusted processes based on dynamic parameters. The governing equations were derived by Timoshenko beam model by energy method. The optimum conditions of the nanocomposite beam- based proposed AIHS are compared with several existing harmony search algorithms. Applying DQ and Hs methods, the optimum values of radius and FS were obtained. The effects of thickness, agglomeration, volume percent of CNTs and boundary conditions were assumed. The results show that with increasing the volume percent of CNTs, the optimum radius of the beam decreases while the FS was improved.

Keywords: harmony search; buckling; optimization nanocomposite beam; nanoparticles

1. Introduction

Nanocomposite structures are made from a matrix reinforced with nanoparticles for improving the property of the material. Recently, the properties of nanocomposite structures have encouraged researchers to investigate about these materials. These structures have many applications such as producing batteries with greater power output, speeding up the healing process for broken bones, producing structural components with a high strength-to-weight ratio, concrete structures and so on. However, optimization analysis of nanocomposite structures is essential, which is studied in the present paper based on a novel numerical method.

Buckling analysis of composite structures has been presented by many researchers. Bending and local buckling of a nanocomposite beam reinforced by a single-walled carbon nanotube (SWCNT) were studied by Vodenitcharova and Zhang (2006) based on the Airy stress-function method.

Based on the three-dimensional theory of elasticity, free vibration characteristics of nanocomposite cylindrical panels reinforced by single-walled carbon nanotubes (CNTs) were considered by Jam *et al*. (2012). Free vibrations analysis of four-parameter continuously graded nanocomposite cylindrical panels reinforced by randomly oriented straight and local aggregation single-walled carbon nanotubes (CNTs) were presented by Pourasghar *et al*. (2013). Pourasghar and Kamarian (2013) presented dynamic behavior of a non-uniform column reinforced by single-walled carbon nanotubes resting on an elastic foundation and subjected to follower force. Free vibration

and the buckling (mechanical and/or thermal) behaviour of laminated composite flat and curved panels were analyzed by Panda and Katariya (2015). Kolahchi *et al*. (2015) investigated nonlocal nonlinear buckling analysis of temperature-dependent microplates reinforced with FG-SWCNT resting on an elastic matrix as orthotropic temperature-dependent elastomeric medium. Based on harmonic differential quadrature (HDQ), Mehri *et al*. (2016) analyzed buckling and vibration responses of a composite truncated conical shell with embedded SWCNTs subjected to an external pressure and axial compression simultaneously. Buckling and vibration analysis of cantilever functionally graded (FG) beam that reinforced with carbon nanotube (CNT) were presented by Nejati *et al*. (2016). Based on DQM and Bolotin's method, Kolahchi *et al*. (2016b) investigated nonlinear dynamic buckling analysis of embedded temperature-dependent viscoelastic plates reinforced by SWCNTs. Katariya and Panda (2016) studied thermal buckling of aminated curved structure of different geometries using higher-order shear deformation theory. Mosharrafian and Kolahchi (2016) presented buckling analysis of classical piezoelectric polymeric cylindrical shell reinforced by armchair double walled boron nitride nanotubes (DWBNNTs). The free vibration and linearized buckling analysis of laminated composite plates were studied using the Isogeometric approach (IGA) and Carrera's Unified Formulation (CUF) (Alesadi *et al*. 2017). Nonlinear thermal buckling load parameter of the laminated composite panel structure was investigated numerically using the higher-order theory by Katariya *et al*. (2017). Zamanian *et al*. (2017) investigated buckling of an embedded straight concrete columns reinforced with silicon dioxide (SiO2) nanoparticles based on Euler- Bernoulli and Timoshenko beam models. Thermal buckling strength of the sandwich shell panel structure and subsequent improvement of the same by embedding shape memory alloy (SMA) fibre via a general higher-order mathematical

---

∗Corresponding author, Ph.D.
 E-mail: mohsen.motezaker@gmail.com

model was presented by Katariya *et al*. (2017). The nonlinear buckling of straight concrete columns armed with SWCNTs resting on foundation was investigated by Bilouei *et al*. (2018) using DQM. Khelifa (2018) studied buckling analysis with stretching effect of functionally graded carbon nanotube-reinforced composite beams resting on an elastic foundation. The eigenfrequency responses of a nanoplate structure were evaluated numerically by Mehar *et al*. (2018) via a novel higher-order mathematical model and finite-element method including nonlocal elasticity theory. Benahmed *et al*. (2019) presented an efficient higher-order nonlocal beam theory for the Critical buckling, of functionally graded (FG) nanobeams with porosities. Numerical buckling analysis of graded CNT-reinforced composite sandwich shell structure under thermal loading was presented by Mehar *et al*. (2019).

However, to date, no research about the buckling optimization of nanocomposite beam with mathematical models has been found in the literature. For the first time, optimization analysis of embedded ZnO nanoparticles reinforced beams under the buckling constraint is presented in this present work. The embedded nanocomposite sinusoidal beams reinforced by ZnO nanoparticles can be optimized based on an improve version of the harmony search optimization method. The SSDT is used for modeling of structure and the corresponded governing equations are derived by energy method and Hamilton's principal. Using and exact solution, the buckling load of structure is calculated and the optimum design conditions are studied using adaptive improved harmony search. Finally, the effects of the axial forces, applied voltage, volume fraction of ZnO nanoparticles, spring constant and shear constant of foundation on the optimum conditions for nanocomposite reinforced sinusoidal beams are evaluated.

2. The harmony search optimization algorithms

The HS has been conceptualized from the musical process of searching a perfect state (global optimum). The harmony quality is enhanced practice after practice, just as the solution quality is enhanced iteration by iteration. The perfect harmony and improvisation group are respectively corresponding to the global optimum and design variables. The HS can be searched the optimum conditions for an optimization engineering problem with several local minima and discontinuation, more accurately. The HS algorithm in clues five basic steps to search the optimal conditions (Bilouei *et al*. 2018):

1) Define the optimization model and HS parameters
2) Determine the initial values of harmony memory
3) Create a new HM
4) Update the harmony memory
5) Check the stopping criterion: Terminate when the maximum number of improvisation is reached.

The optimization processes of harmony search algorithm using the above five steps are summarized as follows:

Step 1: Define the optimization problem, initial values and parameters of the algorithm

The optimization mathematical model for the system is given as follows:

$$find \ L^*, h^*, , rho^*$$

$$min \ \ Cost = f(L, h, rho)$$

$$S.t. \ \ P(L, h, rho, V \ 0) \geq P_{cr} \tag{1}$$

$$0.05 \leq L \leq 5nm, \ 0.05 \leq h \leq 2nm,$$

$$0.05 \leq rho \leq 0.5$$

To search the optimum of objective function, the sets of design variables are randomly generated based on the parameters of harmony search whose are the Harmony Memory Size (HMS), Harmony Memory Considering Rate (*HMCR*), Pitch Adjusting Rate (*PAR*), Total Number of Iteration (maximum of improvisation: *NI*), and bandwidth (*bw*). Each generated harmony memory (HM) are randomly improvised using the parameters of HS including such as *HMCR*, *PAR*, and *bw* based on three rules: 1) consideration of the previous HM members, 2) adjustment of the existing HM, 3) random selection of each member of HM. *HMCR* shows the selection rate of new HM elements from the previous HM. The *PAR* is similar to the mutation of GA algorithm and adjusts the decision variables, randomly. Hence, theeach new design variable is adjusted by bandwidth with the possibility *PAR* × *HMCR*.

Step 2: Define the HM with respect to harmony memory size (HMS) and random uniform generation from domain of each variable, which is given as follows:

$$x_i^j = x_i^L + r \times (x_i^U - x_i^L) \tag{2}$$

where, $r \in [0,1]$ is a random number. Therefore, each design variable is located on the feasible domain $x_i \in [x_i^L, x_i^U]$. Therefore, the HM matrix is generated as follows:

$$HM = \begin{bmatrix} x_1^1 & x_2^1 & ... & x_{N-1}^1 & x_N^1 & | & f(x^1) \\ x_1^2 & x_2^2 & .... & x_{N-1}^2 & x_N^2 & | & f(x^2) \\ . & . & ... & . & . & | & . \\ x_1^j & x_2^j & ... & x_{N-1}^j & x_N^j & | & f(x^j) \\ . & . & ... & . & . & | & . \\ x_1^{HMS-1} & x_2^{HMS-1} & ... & x_{N-1}^{HMS-1} & x_N^{HMS-1} & | f(x^{HMS-1}) \\ x_1^{HMS} & x_2^{HMS} & ... & x_{N-1}^{HMS} & x_N^{HMS} & | & f(x^{HMS}) \end{bmatrix} \tag{3}$$

In this present paper, the bandwidth for design variables are considered based on the lower and upper bounds of each design variable as

$$bw_i = (x_i^U - x_i^L)/1000 \tag{4}$$

Step 3: Improvise a new HM based on the parameters of HS algorithm.

The memory consideration, pitch adjustment, and randomization are applied to improvise the new HM for each design variable in the standard HS algorithm.

where, x' is the new HM, r, r_1, r_2, r_3 are the random number, which are selected in the range from 0-1. The new HM with probability of *HMCR* is selected from the old HM.

Fig. 1. The schematic view of the nanocomposite beam

Then, the new memory is adjusted with the probability of $PAR \times HMCR$ using the uniform distribution and the bandwidth in Eq. (25). The PAR and bw are considered a constant value for all iterations of HS.

Step 4: Update the HM based on the new objective function ($f(x^{rj})$), if $f(x^{rj})$ has much better optimum than previous objective function ($f(x^{j})$), then HM is updated by new memory and worst decision vector is deleted from the HM.

Step 5: Continue the steps 3 and 4 to achieve a good solution or the maximum number of iteration.

3. Buckling analysis of nanocomposite beam

A polymeric beam reinforced by uniform nanoparticles with the length of L and cross section of $b \times h$ is shown in Fig. 1.

The displacements of an arbitrary point in the Timoshenko beam are (Zamanian *et al.* 2017)

$$u_1(x,z) = U(x) + z\psi(x),$$
$$u_2(x,z) = 0, \tag{5}$$
$$u_3(x,z) = W(x)$$

where ψ is the rotation of beam cross-section.

$$\varepsilon_{xx} = \frac{\partial U}{\partial x} + z\frac{\partial \psi}{\partial x} + \frac{1}{2}\left(\frac{\partial W}{\partial x}\right)^2, \tag{6}$$

$$\gamma_{xz} = \frac{\partial W}{\partial x} + \psi. \tag{7}$$

The stress-strain relations can be written as

$$\sigma_{xx} = C_{11}\varepsilon_x, \tag{8}$$

$$\sigma_{xz} = C_{55}\left[\frac{\partial W}{\partial x} + \psi\right], \tag{9}$$

where C_{11} and C_{55} are elastic constants which can be calculated by Mori-Tanaka model as follows (Kolahchi *et al.* 2016b)

$$C_{11} = k + m, \tag{10}$$

$$C_{55} = m, \tag{11}$$

where

$$k = \frac{E_m\{E_m c_m + 2k_r(1+v_m)[1+c_r(1-2v_m)]\}}{2(1+v_m)[E_m(1+c_r-2v_m)+2c_m k_r(1-v_m-2v_m^2)]}, \tag{12}$$

$$m = \frac{E_m[E_m c_m + 2m_r(1+v_m)(3+c_r-4v_m)]}{2(1+v_m)\{E_m[c_m+4c_r(1-v_m)]+2c_m m_r(3-v_m-4v_m^2)\}}, \tag{13}$$

where c_m and c_r are the volume fractions of the polymer and the nano-fibers, respectively and k_r ، l_r ، n_r ، p_r, m_r are the Hills elastic modulus for the nano-fibers. In addition, E_m and υ_m are the Young's modulus and Poisson's ratio of matrix.

The strain energy of the structure can be expressed as

$$U = \frac{1}{2}\int_0^L \int_A (\sigma_{xx}\varepsilon_{xx} + 2\sigma_{xz}\varepsilon_{xz})\, dAdx \tag{14}$$

Submitting Eqs. (13) to (15) into (22) yields

$$U = \frac{1}{2}\int_0^L \left\{ N_x \frac{\partial U}{\partial x} + M_x \frac{\partial \psi}{\partial x} + \frac{1}{2}N_x\left(\frac{\partial W}{\partial x}\right)^2 + Q_x \frac{\partial W}{\partial x} + Q_x \psi \right\} dx \tag{15}$$

The governing equations of structure can be derived from the Hamilton's principle as

$$\frac{\partial N_x}{\partial x} = 0, \tag{16}$$

$$\frac{\partial Q_x}{\partial x} - \frac{\partial}{\partial x}\left(N_x^M \frac{\partial W}{\partial x}\right) + q = 0, \tag{17}$$

$$\frac{\partial M_x}{\partial x} - Q_x = 0, \tag{18}$$

Based on dimensionless parameters as follows

$$\xi = \frac{x}{L}, \ (\overline{W},\overline{U}) = \frac{(W,U)}{h}, \eta = \frac{h}{L}, \psi = \overline{\psi}, \ \overline{K}_w = \frac{K_w hL}{C_{11}A},$$
$$\overline{G}_p = \frac{G_p}{C_{11}A}, \overline{N}_x^M = \frac{N_x^M}{C_{11}A}, \overline{I} = \frac{I}{AL^2}, C_5 = \frac{C_{55}}{C_{11}}. \tag{19}$$

the governing equations can be rewritten as

$$\frac{\partial^2 \overline{U}}{\partial \xi^2} + \eta \frac{\partial^2 \overline{W}}{\partial \xi^2}\frac{\partial \overline{W}}{\partial \xi} = 0, \tag{20}$$

$$C_5\left[\eta\frac{\partial^3 \overline{W}}{\partial \xi^2} + \frac{\partial \overline{\psi}}{\partial \xi}\right] - \overline{N}_x^M \eta \frac{\partial^2 \overline{W}}{\partial \xi^2} = 0, \tag{21}$$

$$\overline{I}\frac{\partial^2 \overline{\psi}}{\partial \xi^2} + K_s C_5\left[\eta\frac{\partial \overline{W}}{\partial \xi} + \overline{\psi}\right] = 0. \tag{22}$$

Based on DQM, the functions f and their k^{th} derivatives with respect to x can be approximated as (Kolahchi *et al.* 2016a)

$$\frac{d^n f(x_i)}{dx^n} = \sum_{j=1}^N C_{ij}^{(n)} f(x_j) \qquad n = 1,...,N-1, \tag{23}$$

where N is the total number of nodes distributed along the x-axis and C_{ij} is the weighting coefficients, the recursive formula for which can be found in (Kolahchi *et al.* 2016a).
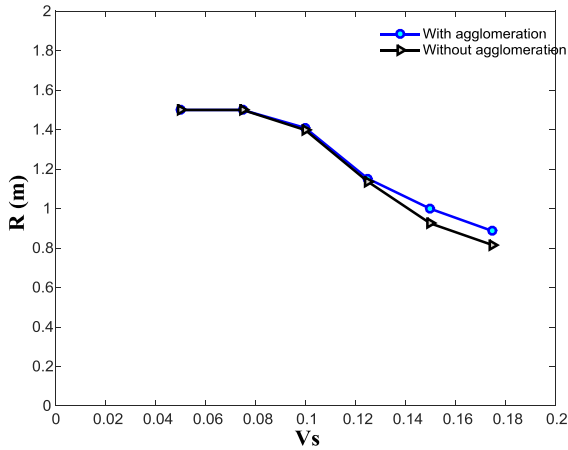
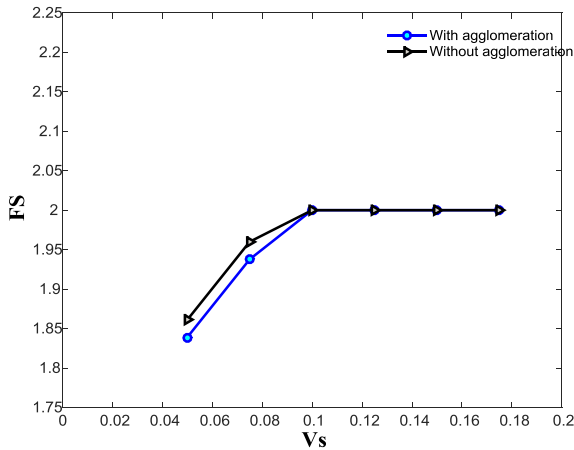Fig. 2 The effect of agglomeration on the optimum radius versus volume percent of CNTs

Fig. 4 The effect of boundary condition on the optimum radius versus volume percent of CNTs

Fig. 3 The effect of agglomeration on the FS versus volume percent of CNTs
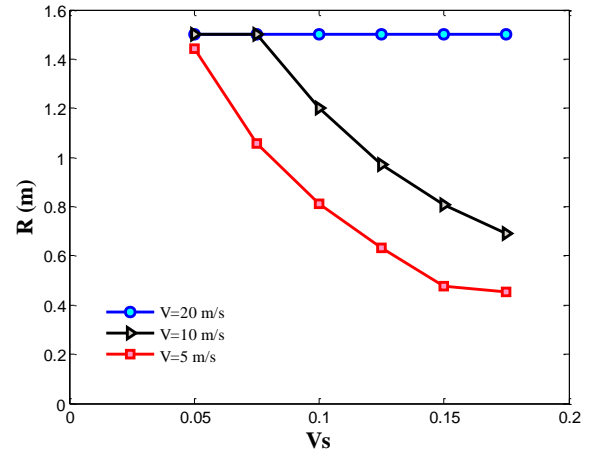
Fig. 5 The effect of boundary condition on the FS versus volume percent of CNTs

Using DQM, the governing equations can be expressed in matrix form as

$$\left(\left[\underbrace{K_L + K_{NL}}_{K}\right] + P[K_g]\right)\begin{Bmatrix}\{d_b\}\\\{d_d\}\end{Bmatrix} = 0, \qquad (24)$$

where K_L is the linear stiffness matrix; K_{NL} is the nonlinear stiffness matrix and K_g is geometric stiffness matrix. Also, d_b and d_d represent boundary and domain points. Finally, based on an iterative method and eigenvalue problem, the buckling load of structure may be obtained.

4. Comparative results and discussions

This section involves three applications of comparing the optimization results based on the proposed HS method. Here, the beam is made from Poly methyl methacrylate (PMMA) with constant Poisson's ratios of $v_m = 0.34$, and Young moduli of $E_m = 3.52 GPa$. The application of HS for optimization of the structure is presented in this section. All codes are written in MATLAB 7.0 and ran on a Intel (R) Core (TM) i5 Laptop with two 2.53 GHz CPU processors
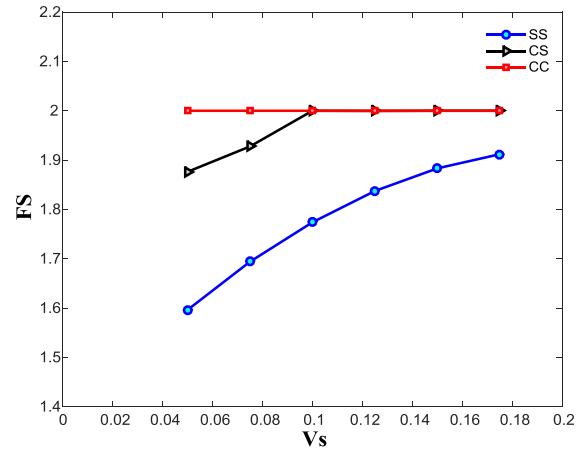
and 4.0 GB RAM memory. The constraint optimization model in Eq. (25) is computed based on an unconstrained cost function (CF) by the penalty method as follows:

$$CF = Cost + \lambda[g(FS)]^\eta \qquad (25)$$

in which, λ and η are the penalty coefficients as $\lambda = 10^8$ and $\eta = 2$. $g(FS)$ is the penalty function, which is computed as follows:

$$g(FS) = \min\{0, FS - 1\} \qquad (26)$$

where *Cost* are the cost to provide the material and *FS* is the safety factor o nanocomposite beam which it can be computed based on the mathematical modeling in Eq. (25).

As shown in Figs. 2 and 3, optimum radius and FS of the structure are plotted versus volume percent of CNTs (*Vs*) in the beam, respectively for agglomeration effects. It can be seen that with increasing the volume percent of CNTs, the optimum radius of the beam decreases while the FS is improved. It is due to the fact that with increasing the volume percent of CNTs, the stiffness of structure increases and however, the optimum radius and FS, respectively, decreases and increases. However, since with increasing the
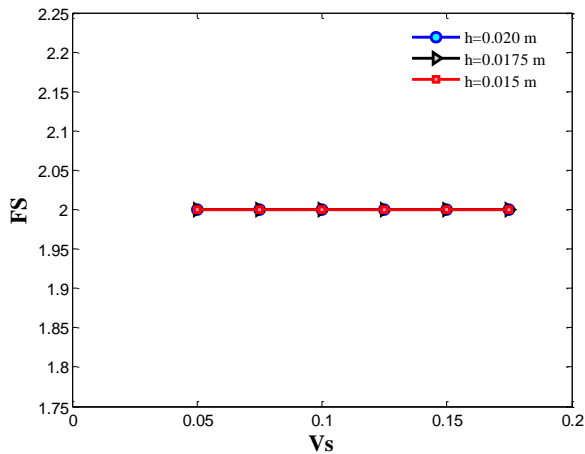
Fig. 6 The effect of beam thickness on the optimum radius versus volume percent of CNTs
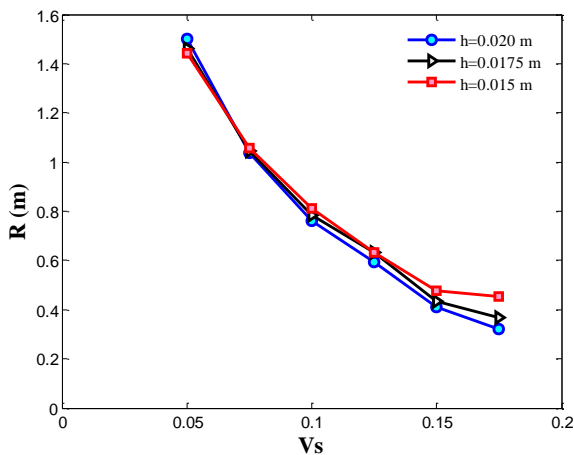

Fig. 7 The effect of beam thickness on the FS versus volume percent of CNTs

volume percent of CNTs, the volume percent of PMMA decreases, the cost of structure becomes lower. In addition, with assuming agglomeration effects, the optimum radius of the beam increases. In other words, assuming agglomeration effects leads to decrease in the safety of the beams due to decrease in the FS.

Figs. 4 and 5 presents the optimum radius and FS versus volume percent of CNTs for different boundary condition, respectively. It is obvious that the optimum radius of the structure is decreased with increasing the volume percent of CNTs while the FS is increased. As an important result, assuming CC boundary condition, the optimum radius of the beam is enhanced while the FS is increased. This physically is logical since assuming CC boundary condition leads to increase in the stability of the beam.

The effects of beam thickness on optimum radius and FS are illustrated in Fig. 6 and 7 with respect to the volume percent of CNTs, respectively. The same as Fig. 6, increasing the volume percent of CNTs leads to decrease in the optimum radius of the structure. It is also concluded that with increasing the beam thickness, the optimum radius of the beam decreases since the stiffness of structure enhances. It is also worth to mention that the beam thickness in the range of 0.015 to 0.02 *m*, does not considerable effect on the FS.

5. Conclusion

In this paper, buckling and optimization of a nanocomposite beam was studied. The agglomeration of nanoparticles was assumed by Mori-Tanaka model. The governing equations were derived by Timoshenko beam model by energy method. Applying DQ and Hs methods, the optimum values of radius and FS were obtained. The effects of thickness, agglomeration, volume percent of CNTs and boundary conditions were assumed. The results show that with increasing the volume percent of CNTs, the optimum radius of the beam decreases while the FS was improved. In addition, assuming agglomeration effects leads to decrease in the safety of the beams due to decrease in the FS. Furthermore, assuming CC boundary condition, the optimum radius of the beam is enhanced while the FS was increased. With increasing the beam thickness, the optimum radius of the beam decreases since the stiffness of structure enhances.

References

Alesadi, A., Galehdari, M. and Shojaee, S. (2017), "Free vibration and buckling analysis of cross-ply laminated composite plates using Carrera's unified formulation based on Isogeometric approach", *Comput. Struct.*, **183**, 38-47. https://doi.org/10.1016/j.compstruc.2017.01.013.

Benahmed, A., Fahsi, B., Benzair, A., Zidour, M., Bourada, F. and Tounsi, A., (2019), "Critical buckling of functionally graded nanoscale beam with porosities using nonlocal higher-order shear deformation", *Struct. Eng. Mech.*, **69**, 457-466. https://doi.org/10.12989/sem.2019.69.4.457.

Bilouei, B.S., Kolahchi, R. and Bidgoli, M.R., (2018), "Buckling of concrete columns retrofitted with Nano-Fiber Reinforced Polymer (NFRP)", *Comput. Concrete*, **18**, 1053-1063. https://doi.org/10.12989/cac.2016.18.5.1053.

Jam, J.E., Pourasghar, A. and Kamarian, S. (2012), "Effect of the aspect ratio and waviness of carbon nanotubes on the vibrational behavior of functionally graded nanocomposite cylindrical panels", *Polym. Compos.*, **33**, 2036-2044. https://doi.org/10.1002/pc.22346.

Katariya, P.V., Panda, S.K. and Mahapatra, T.R. (2017), "Nonlinear thermal buckling behaviour of laminated composite panel structure including the stretching effect and higher-order finite element", *Advan. Mat. Res.*, **6**, 349-361. https://doi.org/10.12989/amr.2017.6.4.349.

Katariya, P.V., Panda, S.K., Hirwani, Ch.K., Mehar, K. and Thakare, O. (2017), "Enhancement of thermal buckling strength of laminated sandwich composite panel structure embedded with shape memory alloy fibre", *Smart Struct. Mat.*, **20**, 595-605. https://doi.org/10.12989/sss.2017.20.5.595.

Khelifa, Z., Hadji, L., Hassaine Daouadji, T. and Bourada, M., (2018), "Buckling response with stretching effect of carbon nanotube-reinforced composite beams resting on elastic foundation", *Struct. Eng. Mech.*, **67**, 125-130.

Kolahchi, R., Bidgoli, M.R., Beygipoor, G. and Fakhar, M.H. (2015), "A nonlocal nonlinear analysis for buckling in embedded FG-SWCNT-reinforced microplates subjected to magnetic field", *J. Mech. Sci. Technol.*, **29**, 3669-3677. https://doi.org/10.1007/s12206-015-0811-9.

Kolahchi, R., Hosseini, H. and Esmailpour, M., (2016a), "Differential cubature and quadrature-Bolotin methods for dynamic stability of embedded piezoelectric nanoplates based on visco-nonlocal-piezoelasticity theories", *Compos. Struct.*,

157, 174-186. https://doi.org/10.1016/j.compstruct.2016.08.032.

Kolahchi, R., Safari, M. and Esmailpour, M., (2016b), "Dynamic stability analysis of temperature-dependent functionally graded CNT-reinforced visco-plates resting on orthotropic elastomeric medium", *Compos. Struct.*, **150**, 255-265. https://doi.org/10.1016/j.compstruct.2016.05.023.

Mehri, M., Asadi, H., and Wang, Q. (2016), "Buckling and vibration analysis of a pressurized CNT reinforced functionally graded truncated conical shell under an axial compression using HDQ method", *Comput. Method. Appl. Mech. Eng.*, **303**, 75-100. https://doi.org/10.1016/j.cma.2016.01.017.

Mehar, K., Mahapatra, T.R., Panda, S.K., Katariya, P.V. and Tompe, U.K. (2018), "Finite-Element Solution to Nonlocal Elasticity and Scale Effect on Frequency Behavior of Shear Deformable Nanoplate Structure", *J. Eng. Mech.*, **144**(9). https://doi.org/10.1061/(ASCE)EM.1943-7889.0001519.

Mehar, K., Panda, S.K., Devarajan, Y. and Choubey, G. (2019), "Numerical buckling analysis of graded CNT-reinforced composite sandwich shell structure under thermal loading", *Compos. Struct.*, **216**, 406-414. https://doi.org/10.1016/j.compstruct.2019.03.002.

Mosharrafian, F., and Kolahchi, R., (2016), "Nanotechnology, smartness and orthotropic nonhomogeneous elastic medium effects on buckling of piezoelectric beams", *Struct. Eng. Mech.*, **58**, 931-947. http://dx.doi.org/10.12989/sem.2016.58.5.931.

Nejati, M., Eslampanah, A., and Najafizadeh, M., (2016), "Buckling and vibration analysis of functionally graded carbon nanotube-reinforced beam under axial load", *J. Appl. Mech.*, **8**, 1650008. https://doi.org/10.1142/S1758825116500083.

Panda, S.K. and Katariya, P.V. (2015), "Stability and free vibration behaviour of laminated composite panels under thermo-mechanical loading", *Int. J. Appl. Computat. Math.*, **1**, 475-490. https://doi.org/10.1007/s40819-015-0035-9.

Pourasghar, A. and Kamarian, S. (2013), "Dynamic stability analysis of functionally graded nanocomposite non-uniform column reinforced by carbon nanotube", *J. Vib. Cont.*, **21**, 2499-2508. https://doi.org/10.1177/1077546313513625.

Pourasghar, A., Yas, M.H. and Kamarian, S. (2013), "Local aggregation effect of CNT on the vibrational behavior of four-parameter continuous grading nanotube-reinforced cylindrical panels", *Polym. Compos.*, **34**, 707-721. https://doi.org/10.1002/pc.22474.

Vodenitcharova, T., and Zhang, L., (2006), "Bending and local buckling of a nanocomposite beam reinforced by a single-walled carbon nanotube", *J. Solids Struct.*, **43**(10), 3006-3024. https://doi.org/10.1016/j.ijsolstr.2005.05.014.

Zamanian, M., Kolahchi, R., and Bidgoli, M.R., (2017), "Agglomeration effects on the buckling behaviour of embedded concrete columns reinforced with SiO2 nano-particles", *Wind Struct.*, **24**, 43-57. https://doi.org/10.12989/was.2017.24.1.043.

CC